Published in final edited form as:
Nanomedicine. 2011 December ; 7(6): 965–974. doi:10.1016/j.nano.2011.04.007.

Intraperitoneal photodynamic therapy mediated by a fullerene in a mouse model of abdominal dissemination of colon adenocarcinoma

Pawel Mroz, MD, PhD[1,2], **Yumin Xia, MD PhD**[1,3], **Daisuke Asanuma, PhD**[1,4], **Aaron Konopko, BS**[1,5], **Timur Zhiyentayev, BS**[1,6], **Ying-Ying Huang, MD**[1,2,7], **Sulbha K Sharma, PhD**[1], **Tianhong Dai, PhD**[1,2], **Usman J. Khan, BS**[1,8], **Tim Wharton, PhD**[9], and **Michael R Hamblin, PhD**[1,2,5,*]

[1]Wellman Center for Photomedicine, Massachusetts General Hospital, Boston, MA

[2]Department of Dermatology, Harvard Medical School, Boston, MA

[3]Department of Dermatology, Renmin Hospital of Wuhan University, Wuhan, China

[4]Graduate School of Pharmaceutical Sciences, University of Tokyo, Japan

[5]Harvard-MIT Division of Health Sciences and Technology, Cambridge, MA

[6]Division of Chemistry and Chemical Engineering, California Institute of Technology, Pasadena, CA, 91125

[7]Aesthetic and Plastic Center of Guangxi Medical University, Nanning, P. R. China

[8]University of Central Florida

[9]Lynntech Inc, College Station, TX

Abstract

Functionalized fullerenes represent a new class of photosensitizer (PS) that is being investigated for photodynamic therapy (PDT) of various diseases including cancer. We tested the hypothesis that fullerenes could be used to mediate PDT of intraperitoneal (IP) carcinomatosis in a mouse model. In humans this form of cancer responds poorly to standard treatment and manifests as a thin covering of tumor nodules on intestines, and other abdominal organs. We used a colon adenocarcinoma cell line (CT26) stably expressing luciferase to allow monitoring of IP tumor burden in BALB/c mice by non-invasive real-time optical imaging using a sensitive low light camera. IP injection of a preparation of N-methylpyrrolidinium-fullerene formulated in Cremophor-EL micelles, followed by white-light illumination delivered through the peritoneal wall (after creation of a skin flap) produced a statistically significant reduction in bioluminescence and a survival advantage in mice.

Correspondence: Prof Michael R Hamblin, Wellman Center for Photomedicine, Massachusetts General Hospital, Boston, MA 02114; Hamblin@helix.mgh.harvard.edu; fax: 617-726-8566.

Conflict of Interest Statement.

At the time of the research Tim Wharton was an employee of Lynntech Inc. Pawel Mroz, Tim Wharton and Michael R Hamblin are inventors on a patent describing the use of fullerenes as photosensitizers for PDT that has been licensed by Lynntech. The Hamblin laboratory has received funding in Phase 1 and 2 SBIR grants awarded to Lynntech.

Keywords

Photodynamic therapy; functionalized fullerene; disseminated abdominal cancer; micellar formulation; hydroxyl radicals

Introduction

The management of serosal surface malignancies, including recurrent peritoneal carcinomatosis resulting from ovarian, gastrointestinal cancers and peritoneal sarcomatosis, is typically palliative in nature (1, 2). Therefore, the development of new effective and safe therapies to address this pattern of cancer spread would be highly significant. One such therapy that has been studied in animal models and in clinical trials is photodynamic therapy (PDT) (3). PDT has the potential to combine selective destruction of cancerous tissue compared to normal tissue with the ability to treat and conform to relatively large surface areas. Moreover, the intrinsic, physical limitation in the depth of visible light penetration through tissue limits PDT damage to deeper structures, thereby providing additional potential for tumor cell selectivity. Intraperitoneal (IP) PDT has shown promise in phase I and II clinical trials of PDT using the first generation photosensitizer (PS) Photofrin (4). However, the toxicity of this treatment was not insignificant and this led to a suboptimal therapeutic index for IP PDT (5, 6).

One possible solution for this problem may be the use of different PS with potentially better therapeutic indices than Photofrin (7). Here we present results showing that a member of a new class of PS, a functionalized fullerene, may be suitable for IP PDT. Fullerenes are a class of closed-cage nanomaterials made exclusively from carbon atoms. A great deal of attention has been focused on developing medical uses of these unique molecules (8). Fullerenes have the ability to generate ROS after illumination with visible light, suggesting a possible role of fullerenes in PDT (9). We have previously shown that N-methylpyrrolidinium-fullerene (BB4) was a powerful PS with an ability to kill cancer cells in vitro after illumination with white light by induction of apoptosis (10). In addition, we have shown that BB4 produces Type I reactive oxygen species (ROS) rather than the more usual Type II ROS, singlet oxygen (10). Because BB4 absorbs strongly between 400–550 nm (blue and green light), its photophysical properties are well suited for applications where controlled necrosis depth (achieved by the reduced tissue penetration of blue and green light compared to red light) is desirable, such as in disseminated peritoneal cancer. There have been reports of a novel technique to deliver light in this wavelength range to deeper tissues that was termed “self-lighting nanoparticles” (11).

In the present study we describe the formulation of BB4 in micelles composed of Cremophor EL and its use *in vitro* and *in vivo* to treat intraperitoneally disseminated colorectal cancer in a mouse model.

Materials and Methods

Photosensitizers and micelle formulation

The synthesis and molecular characterization of BB4 has been previously described in detail (12). The BB4 compound was stored as 2.5-mM solutions in DMSO at room temp in the dark. The UV-visible absorption spectra of the PS were recorded in 1:9 DMSO:water at a concentration of 10 μM using a HP8453 diode array spectrophotometer (Agilent Technologies Inc, Santa Clara, CA). Photofrin was a kind gift from QLT Inc (Vancouver, Canada) and its absorption spectra were taken at 10 μM in PBS.

For *in vitro and vivo* experiments a Cremophor micellar preparation of BB4 was prepared by mixing of 40 μL of 2.5 mM DMSO solution of BB4 with 195 μL of Cremophor EL (BASF, Ludwigshafen, Germany) (100 mg/mL) solution in tetrahydrofuran (THF, 0.3g of Cremophor in 3mL of THF). 1 ml of THF was added to this mixture. The resulting solution was stirred for few minutes until it became one phase and isotropic. The solvent was subsequently removed by rotary evaporation at room temperature. Then the resulting dry film was completely dissolved under sterile conditions in 1 mL of sterile 5% dextrose solution (5DW) to give a solution containing 100 μg BB4 and 20 mg Cremophor; this was then used for PDT studies. Photofrin in 5DW was used as a comparison photosensitizer in vitro.

Light source

We used a Lumacare lamp (Newport Beach, CA) fitted with a light guide fitted with a band-pass filter (400–700 nm) for white light, a 515–555 nm band-pass filter for green light, or a 620–650 nm band-pass filter for red light (see Figure 1C for output spectra). The light guides were adjusted to give a uniform spot of 3 cm diameter with an irradiance of 150 mW/cm^2 as measured with a power meter (model DMM 199 with 201 Standard head, Coherent, Santa Clara, CA).

The emission spectra of the three LumaCare filters were measured using a spectro-radiometer (SPR-01, Luzchem Research Inc., Ottawa, Canada). The detectable spectral range of the spectro-radiometer was 235–850 nm.

Cell lines and culture conditions

We used a colon adenocarcinoma cell line (CT26) (13) (ATCC, Manassas, VA) genetically modified to stably express luciferase called here CT26Luc. CT26Luc cell line was kindly provided by Dr. Andrew Kung from Department of Pediatric Oncology, Dana-Farber Cancer Institute, Boston, MA. VSVG-pseudotyped retrovirus was packaged by triple transfection of pLNCX-neo, pMD-MLV, and pMD-G (Richard Mulligan, HHMI, Boston, MA) into 293T cells. CT26 cells were infected with filtered retroviral stocks at a multiplicity of infection of 10 in the presence of 8 μg/ml of polybrene. The CT26Luc cells were cultured in RPMI medium with L-glutamine and $NaHCO_3$ supplemented with10% heat inactivated fetal bovine serum, penicillin (100 U/mL) and streptomycin (100 μg/mL) (Sigma, St Louis, MO) at 37°C in 5% CO_2 humidified atmosphere in 75cm^2 flasks (Falcon, Invitrogen, Carlsbad, CA). Additionally 500 μg/mL of G418 antibiotic (Sigma, St Louis, MO) was added in order to maintain constant expression of the vector.

ROS studies with probes

3'-(*p*-aminophenyl) fluorescein (APF), 3'-(*p*-hydroxyphenyl) fluorescein (HPF) and Singlet oxygen sensor green (SOG) were purchased from Invitrogen (Carlsbad, CA). APF and HPF were received as stock solutions in DMF and SOG as a solid, which was dissolved in methanol. Probes were stored in the dark and at the recommended temperatures. Solutions for the assay were prepared in flat-bottom 96-well plates (Fisher Sci, Pittsburgh, PA) in quadruplicate and mixed well before fluorescence quantification. Solutions contained 10μM APF, HPF, or SOG with 10μM BB4 or Photofrin. The fluorogenic response of the probe was measured after delivery of 635 nm light (LumaCare) at increasing fluences of 0, 5, 10, 15 and 20 J/cm^2 in a SpectraMax M5 (Molecular Devices, Sunnyvale, CA) plate reader at the appropriate wavelengths for each probe. Red light was employed because the probes (HPF, APF, SOG) can be activated by white (or green) light in the absence of PS.

In vitro studies of phototoxicity

When the cells reached 80% confluence, they were washed with PBS and harvested with 2 mL of 0.25% trypsin-EDTA solution (Sigma). Cells were then centrifuged and counted in trypan blue to ensure viability and plated at density of 5000/well in flat-bottom 96 well plates. Cells were allowed 24h to attach. On the following day dilutions of the fullerenes from DMSO stock solution or in Cremophor as well as Photofrin in 5DW were prepared in complete RPMI medium and added to the cells for 24h incubation. Prior to illumination the PS solution was removed and fresh complete medium was replaced and the illumination (150 mW/cm^2 white light or 635nm red light) was performed. The light spot covered 4 wells which were considered as one experimental group. All wells in a group were illuminated at the same time. The absolute control, DMSO control, Cremophor control and light control groups received; nothing, DMSO (0.0032%), Cremophor (2 mg/mL) and light (maximal fluence) respectively. Following PDT treatment the cells were returned to the incubator overnight and the phototoxicity was measured using a 4h MTT assay read at 560 nm using a microplate spectrophotometer (Spectra Max 340 PC,). An alternative assay for phototoxicity was carried out by measuring bioluminescence intensity 24h after light delivery, using cell lysis and addition of luciferin (Luciferase assay system, Promega Corp, Madison, WI) using a bioluminescence plate reader (MicroBeta Trilux Model 1450, Wallac-Perkin-Elmer, Waltham, MA). Each experiment was repeated 2–4 times.

Mouse model of disseminated cancer

All experiments were carried out according to a protocol approved by the Subcommittee on Research Animal Care (IACUC) at MGH and were in accord with NIH guidelines. Male BALB/c mice (6–8 weeks old) were purchased from Charles River Laboratories (Boston MA). Mice were inoculated with 300,000 CT26-Luc cells suspended in 1ml of PBS into peritoneal cavity. Tumor burdens were calculated based on bioluminescence readings. Fullerenes were injected on day 2 (24 hour drug-light interval) or on day 3 (24 hour drug-light interval) and total abdominal cavity irradiation for PDT was performed on day 3.

Bioluminescence imaging

An ICCD photon-counting camera (Model C2400-30H; Hamamatsu Photonics, Bridgewater, NJ) was used for bioluminescence imaging. The camera was mounted in a light-tight specimen chamber, fitted with a light-emitting diode, a set-up that allowed for a background gray-scale image of the entire mouse to be captured. By accumulating images containing binary photon information (an integration time of 2 minutes was used), a pseudo-color luminescence image was generated. Superimposition of this image onto the gray-scale background image yielded information on the location and intensity in terms of photon number. The camera was also connected to a computer system through an image processor (Argus-50, Hamamatsu Photonics). Argus-50 control program (Hamamatsu Photonics) was used to acquire images and to process the image data collected.

Prior to imaging, mice were anesthetized by i.p. injections of 87.5 mg/kg of ketamine and 12.5 mg/kg xylazine. Mice were then injected with 50mg/kg of luciferin (Gold Biotechnology, St Louis, MO) dissolved in PBS and placed on their backs on an adjustable stage in the specimen chamber directly under the camera. A gray-scale background image of each mouse was made followed by a photon count. This entire photon count was quantified as relative luminescence units (RLUs) and was displayed in a false color scale ranging from pink (most intense) to blue (least intense).

Intraperitoneal Photodynamic Therapy (IPPDT)

The mice bearing CT26-luc tumors were injected IP with 5 mg/kg (1 mL per mouse) of BB4 in Cremophor/5DW. Fullerenes were injected on day 2 (24 hour drug-light interval) or on day 3 (3 hour drug-light interval) and total abdominal cavity irradiation for PDT was performed on day 3 after tumor cell injection. Control mice received Cremophor only. Before illumination mice were anaesthetized with IP injection of 87.5 mg/kg of ketamine and 12.5 mg/kg xylazine and the hair in the abdominal region was shaved and then depilated completely. Under the sterile conditions an abdominal skin flap (see Figure 3A) was surgically created to expose the parietal peritoneal wall. Drops of saline were used to keep the tissue moist. Immediately prior to irradiation each mouse received IP injection with 2 mL of 0.1% Intralipid (Baxter International Inc., Deerfield, IL). White (400 nm-700 nm), green (540 nm) or red (635 nm) light was used to irradiate the exposed region of the abdominal wall. A total fluence of 100 J/cm^2 was delivered at a fluence rate of 100 mW/cm^2. Immediately after irradiation the skin flap was closed and sutured in place. A transparent adhesive film dressing (Tegaderm, 3M Health Care Company, St. Paul, MN, USA) was used to cover the area.

Histology studies

To determine the extent of apoptotic or necrotic cell death in PDT treated tumor tissue a FragEL™ DNA fragmentation (TUNEL) detection kit (KlenowEL DNA®, Calbiochem/EMD4Biosciences, Gibbstown, NJ) was used. Intraperitoneal tumor samples were harvested 24h after PDT, fixed in 10% formalin and embedded in paraffin using standard histology protocol. Tissue sections of 2–4 μm thickness were cut and TUNEL staining was performed according to manufacturer's protocol. Additional pre-treatment with DNAse was used as a positive control. A glass cover slip was mounted over the specimen using DPX mounting media and the images were analyzed with microscopy (Axiophot, Carl Zeiss Microscopy, Thornwood, NY). Additional slides were stained for H&E according to standard protocol.

Statistics

Mean values of bioluminescence RLU were compared with 1-way ANOVA (Microsoft Excel) and Kaplan-Meier survival curves were compared with a log-rank test using the website http://bioinf.wehi.edu.au/software/russell/logrank/ provided by the Walter and Eliza Hall Institute of Biomedical Research Bioinformatics Center. P values less than 0.05 were considered significant.

Results

BB4 mediates PDT via type I and type II mechanisms

We have previously shown that BB4 (see structure Figure 1A) can produce superoxide as well as singlet oxygen (10). The ability of BB4 to produce different reactive oxygen species was monitored using SOG, HPF and APF fluorescence probes in order to better understand the relative contribution of each ROS to PDT effectiveness. It is known that SOG is relatively specific for singlet oxygen ($^1O_2$), HPF is relatively specific for hydroxyl radical (HO•), while APF is sensitive to both $^1O_2$ and HO• (14). It is also known that the probes can to some extent be activated by light in the wavelength range that they absorb (peak at 510-nm) (15); this means that white or green light should not be used to activate the PS in these experiments. Therefore we used red light even though it can be seen from the absorption spectra of both PS (Figure 1C) that this wavelength is sub-optimal. The results from BB4 were contrasted with the ROS production by Photofrin (see structure in Figure 1B).

A roughly comparable light-dose-dependent increase in fluorescence from all three probes (SOG, HPF and APF) was observed when BB4 was illuminated, indicating similar abilities

to produce $^1O_2$ and HO• (Figure 1D). However, Photofrin showed a much greater increase of SOG fluorescence in a light dose-dependent manner than BB4, with a lesser contribution from APF and almost no fluorescence signal from HPF (Figure 1E) indicating that Photofrin cytotoxic effects are mainly due to high production of singlet oxygen while BB4 produces a marked proportion of hydroxyl radicals.

Effectiveness of BB4-mediated PDT against CT26-Luc colon adenocarcinoma cells

The effectiveness of BB4 was tested against the mouse colon adenocarcinoma cell line, CT26 that was modified to express luciferase and thereafter named CT26-Luc. In the first *in vitro* experiments we compared the effectiveness of PDT mediated by BB4 dissolved in DMSO as well as formulated for *in vivo* use in Cremophor micelles. There was no dark toxicity after 24h incubation in case of DMSO formulation while the Cremophor BB4 solution led to 10% of killing in dark conditions. Both formulations tested were effective in producing PDT-induced loss of mitochondrial activity in a light dose-dependent manner against CT26-Luc cells (Figure 2A). The Cremophor formulation however, was dramatically more effective giving over two logs of killing (limit of detection of MTT assay) of CT26-Luc cells compared to about 0.5 log of killing for BB4 in DMSO, as measured by mitochondrial activity.

Because we planned to use the luminescence imaging for *in vivo* tumor monitoring it was necessary to show that the loss of bioluminescence signal from CT26-Luc cells correlated with PDT-mediated cytotoxicity as measured by loss of mitochondrial activity in the MTT assay. As can be seen in Figure 2B there were no significant differences between the loss of viability curves determined by both assays.

Comparison of BB4 in Cremophor PDT with Photofrin PDT

In the next set of *in vitro* experiments we compared the effectiveness of BB4 in Cremophor with the cytotoxic effects of PDT mediated by a clinically approved PS, Photofrin. The CT26-Luc cells were irradiated with white and 635 nm red light. As can be seen in Figure 2C BB4-Cremophor mediated PDT with white light was significantly better than Photofrin under identical conditions. When we compared the effectiveness of both PS receiving 635nm red light irradiation the effectiveness of both PS was significantly reduced compared to that seen with white light reflecting the reduced absorption spectrum of both PS in the red region (Figure 1C). Nevertheless, BB4 in Cremophor was still slightly more effective than Photofrin when irradiated with 635nm red light (Figure 2D).

BB4-Cremophor mediated PDT on CT26-Luc mouse colon carcinoma model of IP disseminated cancer

In a set of *in vivo* experiments we used a novel skin flap model to expose the surface of the peritoneal cavity for transperitoneal illumination (Figure 3A). Previously IP PDT in animal models had been carried out using light (green or red) delivered by fiber optics with diffusing tips that had been inserted transcutaneously through the abdominal wall (16, 17). After IPPDT treatment the skin flap was replaced and sutured in place and the mice recovered well from the procedure (Figure 3B). Figure 3C shows the appearance of the exposed intraperitoneal organs and Figure 3D displays the explanted intestines showing the tumor nodules typical of the disease.

The effects of PDT treatment (carried out on day 0 equivalent to day 4 after tumor cell injection) with white light were monitored using a bioluminescence camera and the CT26-Luc tumor model that expresses luciferase protein. The results are shown in Figure 4. Figure 4A (upper panel) shows the appearance of a representative untreated mouse with CT26-Luc tumor lesions and Figure 4A (lower panel) shows the appearance of a representative mouse

with CT26-Luc tumor after PDT mediated by BB4 in Cremophor and white light each captured on days 0, 3, 7, and 11 of the experiment. The bioluminescence signal after injection of luciferin from the CT26-Luc untreated tumor gradually increased from day 0 though days 3, 7 and 11 (as the lesions progressed) in control animals. In the case of PDT treated mice the bioluminescence signal significantly ($P<0.05$) decreased on day 3 compared to that seen on day 0. Although the bioluminescence increased on day 7 it was only about 15% of that seen in untreated mice ($P<0.001$). Similarly on day 11 the luminescence from the treated tumor was still much lower (30%, $P<0.001$) than that seen in untreated tumors. The increase reflected the gradual regrowth of remaining tumor cells that had escaped being killed by BB4-PDT. The dynamics of mean bioluminescence changes are graphically depicted in Figure 4B.

BB4-Cremophor mediated PDT with white light leads to significant survival advantage

We asked a question how a short (3 hours) drug-light interval compared with the long (24 hours) drug light interval employed in the experiments described above. Furthermore we also investigated how different wavelengths of light compared in their effectiveness in this mouse cancer model. Kaplan-Meier analysis of the survival curves is presented in Figures 5A and 5B. In Figure 5A we compared the effects of IP BB4-PDT on mouse survival mediated by green and white light after a 3h drug-light interval. As can be seen only PDT mediated by white light allowed for some survival advantage. In Figure 5B we compared the effectiveness of IP BB-PDT mediated by white, green and red light after 24h incubation with PS. PDT with red light was highly toxic to mice and led to deaths in 2–3 days after treatment ($P<0.001$). We checked that this systemic toxicity was not due to the red light activating some endogenous PS in the mouse abdomen by repeating the red light study with injection of Cremophor alone (no BB4). Mice showed no toxicity but also no response of tumor after transperitoneal red light alone (data not shown). PDT mediated by green light after 24h post PS administration allowed for some survival advantage while PDT with white light was able to significantly prolong mice survival for over 7 days compared to control. The p values of the log-rank test comparisons are shown in Table 1.

IP BB4-PDT with white light leads to significant necrosis within peritoneal tumor lesions

To better understand the differences in the effectiveness of different light wavelengths we sacrificed some of PDT treated mice to harvest the intraperitoneal lesions. Figure 3C shows a picture of intraperitoneal lesions growing within intestine loops in the abdominal cavity. We isolated colon loops with tumor lesions (Figure 3D) and subsequently processed selected samples for histology.

The histological analysis by H&E staining revealed tumor formation in case of untreated control animals (Figure 6A) while PDT with green and white light led to different degree of tissue damage (Figure 6 B & C respectively). The white light treated sample showed the most pronounced PDT related tissue damage, while the green light PDT led to only slight damage within tumor lesions. It can be seen that in case of white light the damage to tumor lesion is significant and suggestive of necrosis. To further investigate the mode of death in the observed tissue damage areas we used TUNEL staining to assay for apoptosis and compare it with DNAse treatment of the same samples for a positive control. The untreated control sample pre-treated with DNAse (Figure 6D) stained almost homogenously, while the green light PDT treated sample (Figure 6E) revealed a mixture of apoptosis and necrosis on the outskirts of the lesion with a strongly necrotic tumor center. The white light PDT (Figure 6F) led to almost no apoptotic cells within the lesion. Those findings were in marked contrast with the lack of significant staining in DNAse negative sections. The relatively low staining signal from control section (Figure 6G) confirms high viability of non-treated control lesions while the lack of TUNEL staining after PDT with green (Figure 6H) and

white light (Figure 6I) confirms the impressions from H&E histology that necrosis rather than apoptosis was the main mode of cell death in vivo after IP BB4-PDT. It can be also seen that within the necrotic areas there are islands of surviving cells grouped around tumor vessels that may be responsible for tumor regrowth.

Discussion

The discovery of fullerenes in 1985 (18) has been hailed as the beginning of the nanotechnology revolution. Many groups have attempted to demonstrate whether fullerenes have a role to play in biomedical therapy (19–22). Using fullerenes as PS for mediating PDT of cancer is a relatively new approach (9). We have shown in the present report that not only can a fullerene be active in PDT of an animal model of cancer, but that BB4 and white light can also give significant anti-cancer therapeutic benefit in the highly challenging model of disseminated peritoneal carcinomatosis in the mouse.

We had previously shown that BB4 formulated from DMSO into culture medium could be effective in mediating *in vitro* PDT of cancer cells including CT26 (10). However the pronounced tendency of fullerenes to aggregate prompted us to consider formulating BB4 in Cremophor micelles. This made BB4 at least ten times more effective in mediating PDT *in vitro* and allowed us to use this formulation in our *in vivo* experiments. Many other reports of hydrophobic PS being used as PS for PDT have used Cremophor formulation (23, 24) as well as other different micellar preparations (25).

It has been shown that fullerenes in organic solvents are highly efficient in generating $^1O_2$ (Type 2 mechanism) after light absorption due to their high triplet yield (reaction 1) (26). However when fullerenes are in aqueous solvents or biological environments their photochemistry changes to a Type 1 mechanism typified by generation of superoxide by electron transfer from the fullerene radical anion ($BB4^{\bullet-}$) to ground state oxygen (reactions 2 or 3 and 4) (27). It is not clear exactly why this change in solvent should have a big effect on the photochemical mechanism but it can be hypothesized that may be connected with the tendency of the fullerene to be more aggregated in aqueous and biological environments. There exists evidence that aggregated photosensitizers are more likely to carry out type 1 photochemistry compared with perfectly soluble monomeric forms (28). Another possibility is that different reactions can take place at membrane interfaces (29). It is also at present unclear where the electron comes from in reaction 2 when the photosensitization takes place with the probes in aqueous solution. In biological environments it has been suggested that reducing agents such as NADH and $FADH_2$ may be the source of the electron (30, 31), but in the probes experiments there were no such reducing agents present. Another possibility is that two fullerene molecules in the triplet state (or one in the triplet state and one in the ground state) carry out a single electron transfer to form a pair consisting of a radical anion and a radical cation (eq 3) (32–34). The radical anion can go on to participate in eq 4 while the fate of the radical cation remains uncertain.

Our finding that fullerenes also generate hydroxyl radicals can therefore be explained by the following hypothesized series of reactions.

$$BB4+h\nu \rightarrow {}^3BB4 \quad (1)$$

$$^3BB4+e^{\bullet-} \rightarrow BB4^{\bullet-} \quad (2)$$

$$(\text{or})\ 2\ {}^{3}\text{BB4} \rightarrow \text{BB4}^{\bullet -} + \text{BB4}^{\bullet +} \quad (3)$$

$$\text{BB4}^{\bullet -} + \text{O}_2 \rightarrow \text{BB4} + \text{O}_2^{\bullet -} \quad (4)$$

$$2\ \text{O}_2^{\bullet -} + 2\ \text{H}^{+} \rightarrow \text{O}_2 + \text{H}_2\text{O}_2 \quad (5)$$

$$\text{BB4}^{\bullet -} + \text{H}_2\text{O}_2 \rightarrow \text{BB4} + \text{OH}^{-} + \text{HO}^{\bullet} \quad (6)$$

Although it has not yet been conclusively proven, it is possible that the highly reactive $HO^{\bullet}$ is proportionately more cytotoxic than $^{1}O_2$ on a molecule for molecule basis. Furthermore, it is reasonably well-accepted that type 1 photochemistry is less dependent on the surrounding oxygen concentration than is type 2 photochemistry (35, 36). Fullerenes may be able to be relatively more effective in hypoxic tumors growing in such regions as the peritoneal cavity where pO2 levels are lower than in well-perfused tissues (37).

We devised a new approach to carrying out IP PDT in mice. This was necessitated by the requirement to use white light to maximize light absorption by the fullerene. Collimated laser light can be readily coupled into fiber optics that can be transcutaneously inserted into the abdomen (16, 17), whereas this procedure is not readily feasible with non-coherent white light. However the relatively simple procedure of creating a temporary skin flap to allow light delivery through the transparent abdominal wall was well tolerated by the mice. It should be noted that this procedure would not be feasible in humans due to the presence of a muscle layer covering the abdominal wall. We used bioluminescence imaging combined with tumor cells stably expressing firefly luciferase to monitor tumor growth and quantify tumor burden. This is especially important in cases such as disseminated intraperitoneal tumor where it is impossible to measure tumor dimensions (38, 39). Bioluminescence imaging of disseminated peritoneal tumor has been used to study response to therapies such as radioimmunotherapy with I^{125}-labeled antibodies (40) and conjugates between daidzein and alliinase (41).

We found that red light in combination with IP BB4 produced rapid fatalities amongst the mice due to systemic toxicity that was not found with red light alone. This somewhat surprising finding is presumably due to excessive light penetration into abdominal organs and has been reported by other studies comparing red and green light for IP PDT in small animal models (42).

The predominant observation of necrosis rather than apoptosis as a mode of cell death *in vivo* may be due to direct cellular uptake of the BB4 delivered IP and not uptake mediated by tumor blood vessels. Many reports of apoptosis after PDT *in vivo* have been carried out after PS were injected IV. The histological slides revealed that the surviving tumor cells were grouped around tumor blood vessels suggesting that because the BB4 was administered by IP injection, it did not efficiently reach tumor blood vessels. It could be envisaged that a dual BB4 administration schedule consisting of IP injection with a 24 hour drug-light interval and an IV injection with a short (15 minute) drug-light interval might be able to produce both cellular and vascular PDT and maximize tumor destruction. Such a

dual vascular-cellular targeted PDT regimen mediated by two drug-light intervals of IV injected verteporfin has previously been reported (43).

To our best knowledge there have only been four reports of fullerene-mediated PDT of cancer *in vivo* - three in animal models and one in patients. Tabata et al reported (44) in 1997 that a C_{60}-PEG conjugate injected intravenously into mice carrying a subcutaneous tumor followed by exposure of the tumor site to visible light exhibited a stronger suppressive effect than Photofrin. Liu et al (45) prepared C_{60}-PEG attached to DTPA-Gd and carried PDT out MRI imaging and PDT of subcutaneous tumor s using 500–500-nm light. Chiang and coworkers reported (46), a preliminary in vivo study using hydrophilic nanospheres formed from water-soluble hexa(sulfo-n-butyl)-C_{60} injected either IP or IV followed by illumination 515-nm or 633-nm lasers. Inhibition of tumor growth was more effective using 515nm laser than the 633-nm laser. The first fullerene-based clinical PDT treatment of a human patient with rectal adenocarcinoma was attempted by Andrievsky et al in 2000 (47).

Our laboratory recently published one of the first reports of fullerenes saving the life of mice in a study using a tris-cationic functionalized fullerene to mediate antimicrobial PDT (using white light) of virulent bacteria contaminating an excisional wound (48).

In conclusion we have shown that IP PDT with a fullerene and white light has significant therapeutic effects in a challenging mouse model of disseminated abdominal cancer, and this observation suggests that fullerenes continue to be explored as PS for PDT of cancer and other dread diseases.

Acknowledgments

We are grateful to Dr. Andrew Kung from Department of Pediatric Oncology, Dana-Farber Cancer Institute, Boston, MA for providing CT26Luc cell line.

We are grateful to QLT Inc, Vancouver, Canada for the gift of Photofrin.

Funding.

This work was supported by US NIH grants R43AI68400 to Lynntech Inc and R01AI050875 to M.R.H. and by the US Air Force Medical Free Electron Laser Program (FA9550-04-1-0079). P.M. was partly supported by a Genzyme-Partners Translational Research Grant. T.D. was supported by the Bullock Wellman Postdoctoral Fellowship and an Airlift Research Foundation grant (grant #109421).

References

1. Teo M. Peritoneal-based malignancies and their treatment. Ann Acad Med Singapore. 2010; 39:54–57. [PubMed: 20126816]
2. Cotte E, Passot G, Mohamed F, Vaudoyer D, Gilly FN, Glehen O. Management of peritoneal carcinomatosis from colorectal cancer: current state of practice. Cancer J. 2009; 15:243–248. [PubMed: 19556911]
3. Cengel KA, Glatstein E, Hahn SM. Intraperitoneal photodynamic therapy. Cancer Treat Res. 2007; 134:493–514. [PubMed: 17633077]
4. Hendren SK, Hahn SM, Spitz FR, Bauer TW, Rubin SC, Zhu T, et al. Phase II trial of debulking surgery and photodynamic therapy for disseminated intraperitoneal tumors. Ann Surg Oncol. 2001; 8:65–71. [PubMed: 11206227]
5. Canter RJ, Mick R, Kesmodel SB, Raz DJ, Spitz FR, Metz JM, et al. Intraperitoneal photodynamic therapy causes a capillary-leak syndrome. Ann Surg Oncol. 2003; 10:514–524. [PubMed: 12794017]

6. Hahn SM, Fraker DL, Mick R, Metz J, Busch TM, Smith D, et al. A phase II trial of intraperitoneal photodynamic therapy for patients with peritoneal carcinomatosis and sarcomatosis. Clin Cancer Res. 2006; 12:2517–2525. [PubMed: 16638861]
7. Allison RR, Bagnato VS, Sibata CH. Future of oncologic photodynamic therapy. Future Oncol. 2010; 6:929–940. [PubMed: 20528231]
8. Chawla P, Chawla V, Maheshwari R, Saraf SA, Saraf SK. Fullerenes: from carbon to nanomedicine. Mini Rev Med Chem. 2010; 10:662–677. [PubMed: 20236059]
9. Mroz P, Tegos GP, Gali H, Wharton T, Sarna T, Hamblin MR. Photodynamic therapy with fullerenes. Photochem Photobiol Sci. 2007; 6:1139–1149. [PubMed: 17973044]
10. Mroz P, Pawlak A, Satti M, Lee H, Wharton T, Gali H, et al. Functionalized fullerenes mediate photodynamic killing of cancer cells: Type I versus Type II photochemical mechanism. Free Radic Biol Med. 2007; 43:711–719. [PubMed: 17664135]
11. Chen W, Zhang J. Using nanoparticles to enable simultaneous radiation and photodynamic therapies for cancer treatment. J Nanosci Nanotech. 2006; 6:1159–1166.
12. Tegos GP, Demidova TN, Arcila-Lopez D, Lee H, Wharton T, Gali H, et al. Cationic fullerenes are effective and selective antimicrobial photosensitizers. Chem. Biol. 2005; 12:1127–1135. [PubMed: 16242655]
13. Brattain MG, Strobel-Stevens J, Fine D, Webb M, Sarrif AM. Establishment of mouse colonic carcinoma cell lines with different metastatic properties. Cancer Res. 1980; 40:2142–2146. [PubMed: 6992981]
14. Price M, Reiners JJ, Santiago AM, Kessel D. Monitoring singlet oxygen and hydroxyl radical formation with fluorescent probes during photodynamic therapy. Photochem Photobiol. 2009; 85:1177–1181. [PubMed: 19508643]
15. Price M, Kessel D. On the use of fluorescence probes for detecting reactive oxygen and nitrogen species associated with photodynamic therapy. J Biomed Opt. 2010; 15:051605. [PubMed: 21054079]
16. Lilge L, Molpus K, Hasan T, Wilson BC. Light dosimetry for intraperitoneal photodynamic therapy in a murine xenograft model of human epithelial ovarian carcinoma. Photochem Photobiol. 1998; 68:281–288. [PubMed: 9747583]
17. Molpus KL, Kato D, Hamblin MR, Lilge L, Bamberg M, Hasan T. Intraperitoneal photodynamic therapy of human epithelial ovarian carcinomatosis in a xenograft murine model. Cancer Res. 1996; 56:1075–1082. [PubMed: 8640764]
18. Kroto HW. C60: Buckminsterfullerene. Nature. 1985; 318:162–163.
19. Bosi S, Da Ros T, Spalluto G, Prato M. Fullerene derivatives: an attractive tool for biological applications. Eur J Med Chem. 2003; 38:913–923. [PubMed: 14642323]
20. Dugan LL, Gabrielsen JK, Yu SP, Lin TS, Choi DW. Buckminsterfullerenol free radical scavengers reduce excitotoxic and apoptotic death of cultured cortical neurons. Neurobiol Dis. 1996; 3:129–135. [PubMed: 9173920]
21. Kato S, Aoshima H, Saitoh Y, Miwa N. Fullerene-C60/liposome complex: Defensive effects against UVA-induced damages in skin structure, nucleus and collagen type I/IV fibrils, and the permeability into human skin tissue. J Photochem Photobiol B. 2009
22. Nakamura E, Isobe H. Functionalized fullerenes in water. The first 10 years of their chemistry, biology, and nanoscience. Acc Chem Res. 2003; 36:807–815. [PubMed: 14622027]
23. Decreau R, Richard MJ, Verrando P, Chanon M, Julliard M. Photodynamic activities of silicon phthalocyanines against achromic M6 melanoma cells and healthy human melanocytes and keratinocytes. J Photochem Photobiol B. 1999; 48:48–56. [PubMed: 10205878]
24. Kessel D. Properties of cremophor EL micelles probed by fluorescence. Photochem Photobiol. 1992; 56:447–451. [PubMed: 1454875]
25. Taillefer J, Jones MC, Brasseur N, van Lier JE, Leroux JC. Preparation and characterization of pH-responsive polymeric micelles for the delivery of photosensitizing anticancer drugs. J Pharm Sci. 2000; 89:52–62. [PubMed: 10664538]
26. Arbogast JW, Darmanyan AP, Foote CS, Rubin Y, Diederich FN, Alvarez MM, et al. Photophysical properties of C60. J Phys Chem A Mol Spectrosc Kinet Environ Gen Theory. 1991; 95:11–12.

27. Yamakoshi Y, Umezawa N, Ryu A, Arakane K, Miyata N, Goda Y, et al. Active oxygen species generated from photoexcited fullerene (C60) as potential medicines: O2-* versus 1O2. J.Am.Chem.Soc. 2003; 125:12803–12809. [PubMed: 14558828]
28. Athar M, Mukhtar H, Bickers DR. Differential role of reactive oxygen intermediates in photofrin-I- and photofrin-II-mediated photoenhancement of lipid peroxidation in epidermal microsomal membranes. J Invest Dermatol. 1988; 90:652–657. [PubMed: 2834456]
29. Vakrat-Haglili Y, Weiner L, Brumfeld V, Brandis A, Salomon Y, McLlroy B, et al. The microenvironment effect on the generation of reactive oxygen species by Pd-bacteriopheophorbide. J Am Chem Soc. 2005; 127:6487–6497. [PubMed: 15853357]
30. Martin JP, Logsdon N. Oxygen radicals are generated by dye-mediated intracellular photooxidations: a role for superoxide in photodynamic effects. Arch Biochem Biophys. 1987; 256:39–49. [PubMed: 3038028]
31. Zhao B, Bilski PJ, He YY, Feng L, Chignell CF. Photo-induced reactive oxygen species generation by different water-soluble fullerenes (C) and their cytotoxicity in human keratinocytes. Photochem Photobiol. 2008; 84:1215–1223. [PubMed: 18399919]
32. Chignell CF, Sik RH. Magnetic field effects on the photohemolysis of human erythrocytes by ketoprofen and protoporphyrin IX. Photochemistry and photobiology. 1995; 62:205–207. [PubMed: 7638268]
33. Aveline BM, Sattler RM, Redmond RW. Environmental effects on cellular photosensitization: correlation of phototoxicity mechanism with transient absorption spectroscopy measurements. Photochem Photobiol. 1998; 68:51–62. [PubMed: 9679451]
34. Waliszewski P, Skwarek R, Jeromin L, Minikowski H. On the mitochondrial aspect of reactive oxygen species action in external magnetic fields. J Photochem Photobiol B. 1999; 52:137–140. [PubMed: 10681215]
35. Detty MR, Merkel PB, Gibson SL, Hilf R. Chalcogenapyrylium dyes as dual-action sensitizers for photodynamic therapy. Oncol Res. 1992; 4:367–373. [PubMed: 1336686]
36. Milanesio ME, Alvarez MG, Rivarola V, Silber JJ, Durantini EN. Porphyrin-fullerene C60 dyads with high ability to form photoinduced charge-separated state as novel sensitizers for photodynamic therapy. Photochem Photobiol. 2005; 81:891–897. [PubMed: 15757366]
37. Sawyer RG, Spengler MD, Adams RB, Pruett TL. The peritoneal environment during infection. The effect of monomicrobial and polymicrobial bacteria on pO2 and pH. Ann Surg. 1991; 213:253–260. [PubMed: 1998406]
38. Toyoshima M, Tanaka Y, Matumoto M, Yamazaki M, Nagase S, Sugamura K, et al. Generation of a syngeneic mouse model to study the intraperitoneal dissemination of ovarian cancer with in vivo luciferase imaging. Luminescence. 2009; 24:324–331. [PubMed: 19711487]
39. Buchhorn HM, Seidl C, Beck R, Saur D, Apostolidis C, Morgenstern A, et al. Non-invasive visualisation of the development of peritoneal carcinomatosis and tumour regression after 213Bi-radioimmunotherapy using bioluminescence imaging. Eur J Nucl Med Mol Imaging. 2007; 34:841–849. [PubMed: 17206415]
40. Boudousq V, Ricaud S, Garambois V, Bascoul-Mollevi C, Boutaleb S, Busson M, et al. Brief intraperitoneal radioimmunotherapy of small peritoneal carcinomatosis using high activities of noninternalizing 125I-labeled monoclonal antibodies. J Nucl Med. 2010; 51:1748–1755. [PubMed: 20956481]
41. Appel E, Rabinkov A, Neeman M, Kohen F, Mirelman D. Conjugates of daidzein-alliinase as a targeted pro-drug enzyme system against ovarian carcinoma. J Drug Target. 2010
42. Veenhuizen RB, Ruevekamp MC, Oppelaar H, Ransdorp B, van de Vijver M, Helmerhorst TJ, et al. Intraperitoneal photodynamic therapy: comparison of red and green light distribution and toxicity. Photochem Photobiol. 1997; 66:389–395. [PubMed: 9297983]
43. Chen B, Pogue BW, Hoopes PJ, Hasan T. Combining vascular and cellular targeting regimens enhances the efficacy of photodynamic therapy. Int J Radiat Oncol Biol Phys. 2005; 61:1216–1226. [PubMed: 15752904]
44. Tabata Y, Murakami Y, Ikada Y. Photodynamic effect of polyethylene glycol-modified fullerene on tumor. Jpn.J.Cancer Res. 1997; 88:1108–1116. [PubMed: 9439687]

45. Liu J, Ohta S, Sonoda A, Yamada M, Yamamoto M, Nitta N, et al. Preparation of PEG-conjugated fullerene containing Gd3+ ions for photodynamic therapy. J Control Release. 2007; 117:104–110. [PubMed: 17156882]

46. Chi Y, Canteenwala T, Chen HC, Chen BJ, Canteenwala M, Chiang LY. Hexa(sulfobutyl)fullerene-induced photodynamic effect on tumors in vivo and toxicity study in rats. Proc Electrochem Soc. 1999; 99:234–249.

47. Andrievsky, G.; Zhmuro, A.; Zabobonina, L.; Suchina, E. Biochemical and Pharmaceutical Aspects of Fullerene Materials. Toronto, Canada: 2000. First clinical case of treatment of patient (volunteer) with rectal adenocarcinoma by hydrated fullerenes: Natural course of the disease or non-specific anticancer activity?. Poster presentation No. 0377

48. Lu Z, Dai T, Huang L, Kurup DB, Tegos GP, Jahnke A, et al. Photodynamic therapy with a cationic functionalized fullerene rescues mice from fatal wound infections. Nanomedicine (UK). 2010; 5:1525–1533.

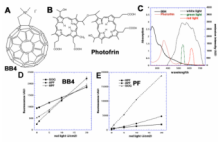

Figure 1.

(A) Chemical structure of BB4. (B) Chemical structure of Photofrin. (C) UV-visible absorption spectra of BB4 in DMSO:water 1:9 (black solid), Photofrin in PBS (red solid) and filter emission spectra for broadband white (black dashes), 540 nm green (green dashes) and 635 nm red (red dashes). (D) Fluorescence generated from ROS probes, HPF, APF and SOG (10 μM) and BB4 (10 μM) illuminated with 630-nm light. (E) Similar probes with Photofrin (10μM).

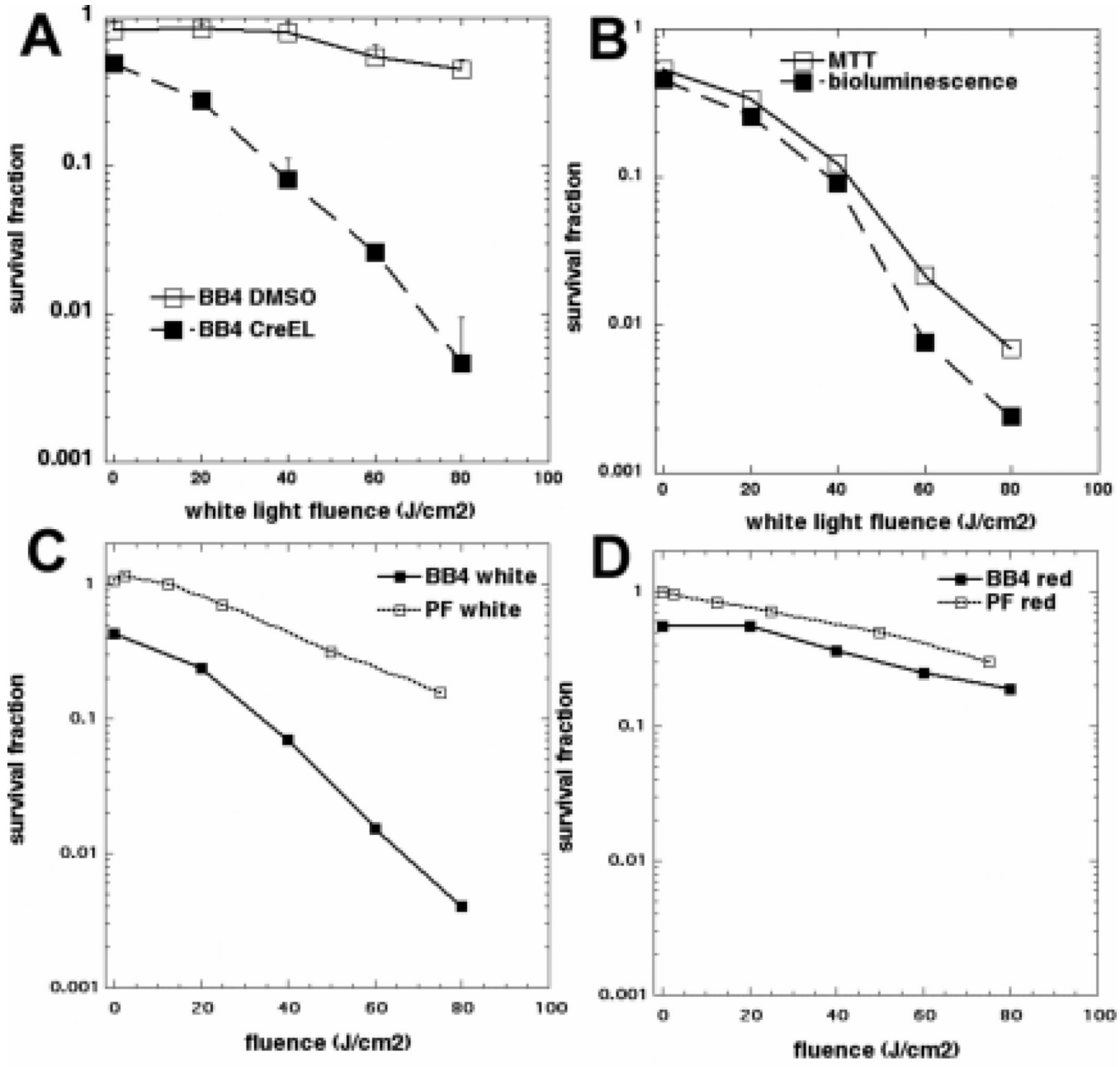

Figure 2.

(A). Broad-band white light-fluence dependent inactivation of mitochondrial activity of CT26-Luc cells after 24h incubation with 2 μM BB4 from DMSO or Cremphor stocks. (B). Comparison of the effectiveness of PDT with white light mediated by BB4 in Cremophor against CT26-Luc cells measured by inactivation of mitochondrial activity and loss of bioluminescence signal. (C). Comparison of PDT effectiveness (MTT assay) against CT26-Luc cells with BB4 in Cremophor and Photofrin (PF) after white light irradiation and (D) after 635nm red light irradiation.

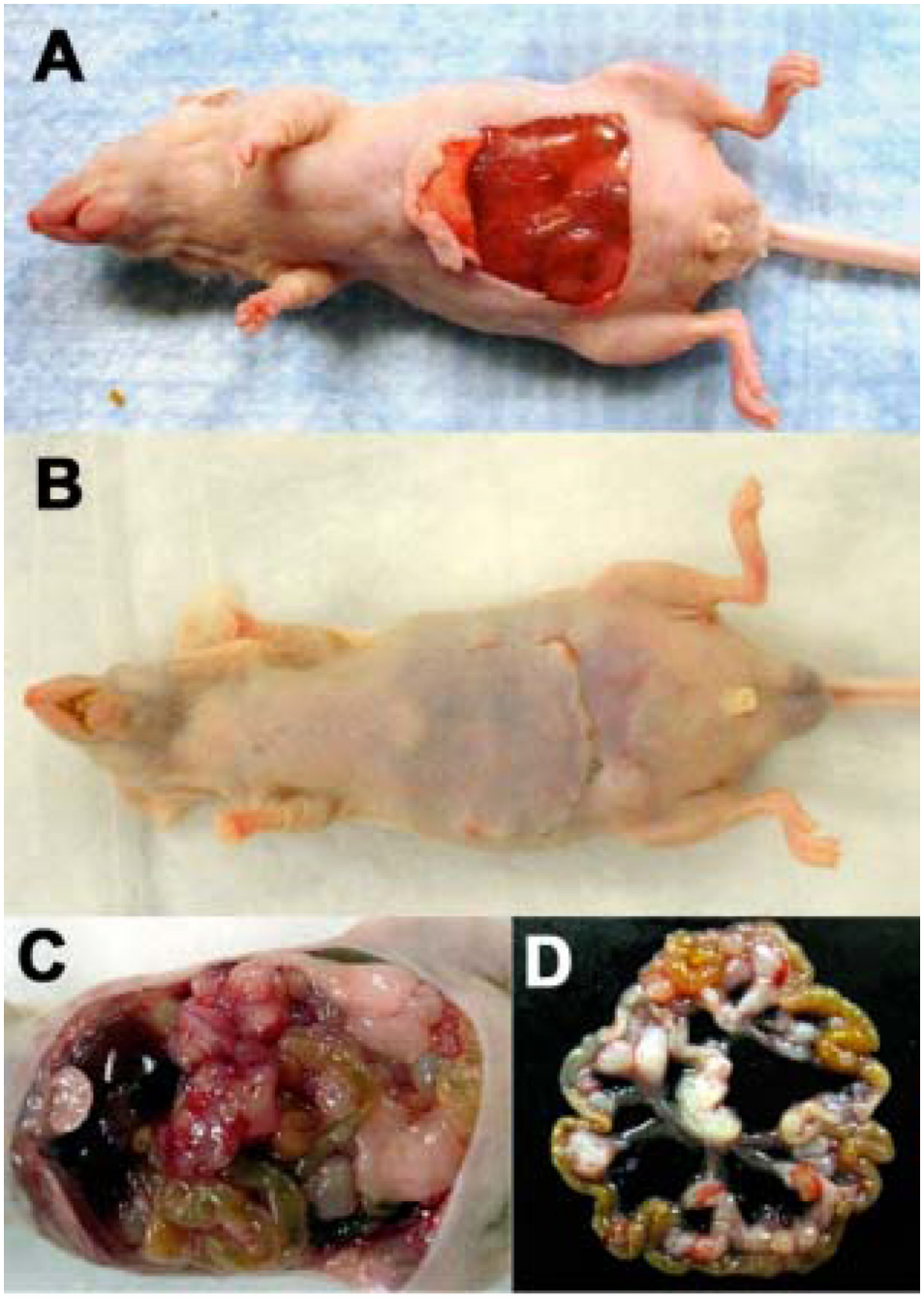

Figure 3.

(A). Photograph of mouse prepared for transperitoneal illumination of intraperitoneal CT26-Luc lesions. A skin flap was created to expose peritoneal surface and underlying abdominal organs. (B). Mouse recovering after repositioning of the skin flap and suturing after light irradiation. (C). Intraperitoneal disseminated lesions of CT26-Luc in mouse abdomen. (D). Isolated loop of mouse colon with several CT26-Luc tumor lesions after IP PDT.

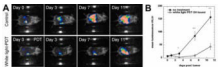

Figure 4.

(A). Bioluminescence imaging of CT26-Luc tumors growing in a representative control mouse (upper panel) and a representative IP PDT treated mouse (lower panel). (B). Quantitative analysis of bioluminescence dynamics in control and white light treated mice (n=10 per group). * $P < 0.05$; ** $P < 0.001$.

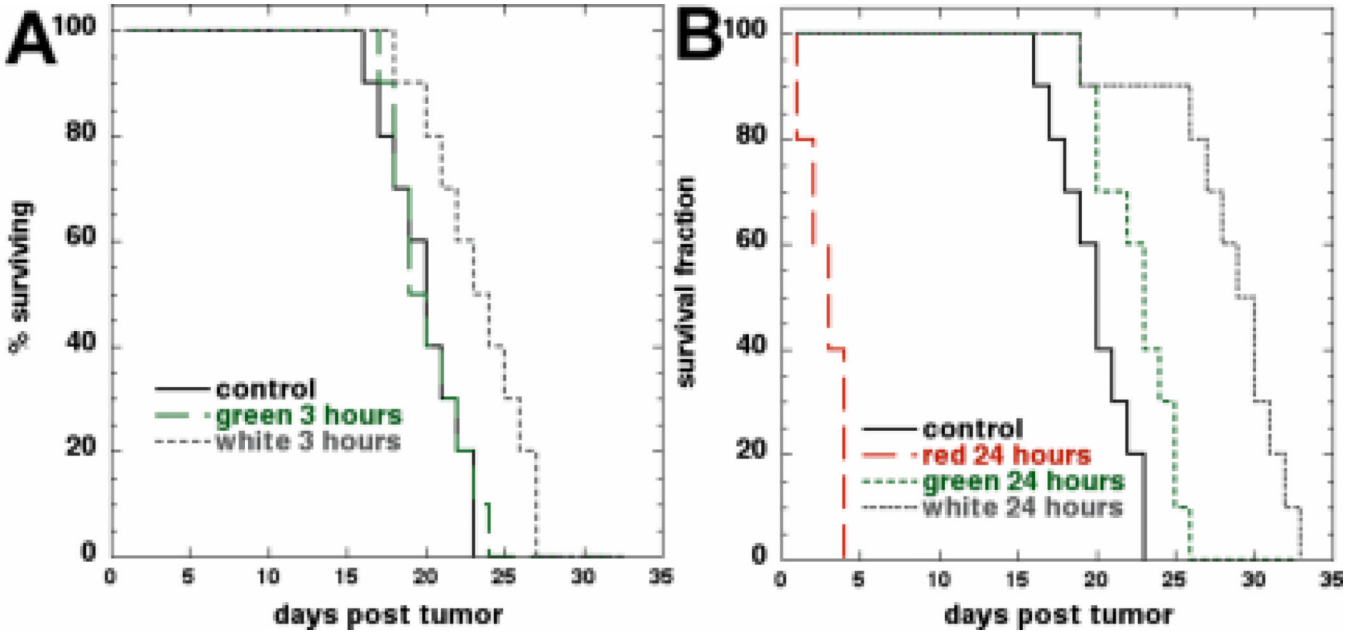

Figure 5.

Kaplan-Meier survival curves (n=10 per group). Control mice received Cremophor but no light treatment. (A). Mice subjected to 540-nm green or broad band white light irradiation 3h after administration of BB4 in Cremophor. (B). Mice irradiated with broad band white light, 540-nm green light or 635-nm red light 24h after administration of BB4 in Cremophor.

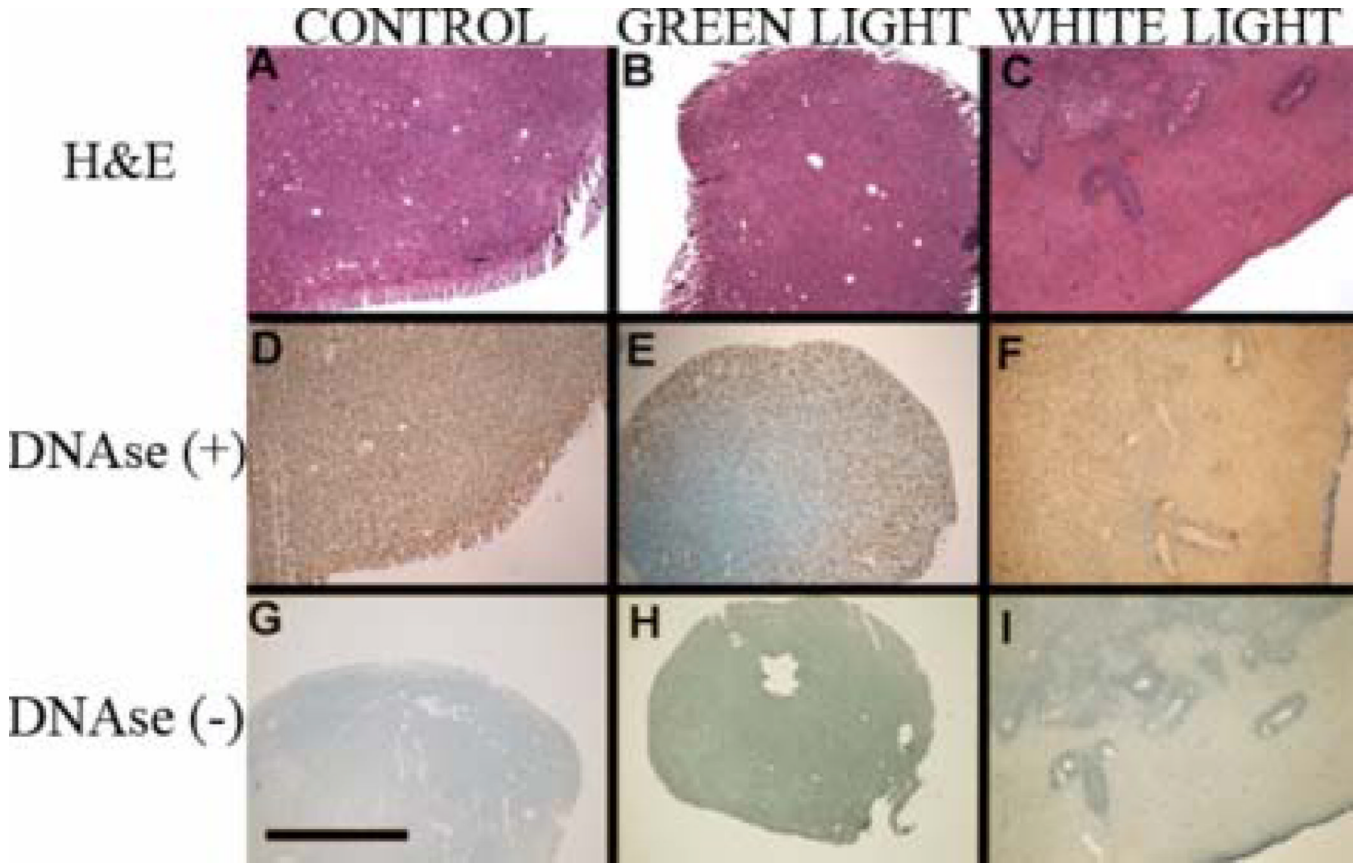

Figure 6.
Histological staining for H&E (A, B, C) as well as TUNEL with DNAse (D, E, F positive control) or without DNAse (G, H, I) of sections from tumor samples treated with control (A, D, G), PDT using green light (B, E, H) and PDT using white light (C, F, I). Scale bar = 1 mm.

Table 1

Statistical comparisons of survival times after IP PDT

	Control	White 24h	White 3h	Green 24h	Green 3h
Control	X				
White 24 h	7.24e-5	X			
White 3 h	0.00972	0.000792	X		
Green 24 h	0.0215	0.00017	n.s.	X	
Green 3 h	n.s.	4.08e-5	0.0129	0.0259	X

A log rank test was carried out on survival data from Figures 4A and 4B using the website http://bioinf.wehi.edu.au/software/russell/logrank/ provided by the Walter and Eliza Hall Institute of Biomedical Research Bioinformatics Center and the relevant P values are shown